3-2000

Infrared Spectroscopy of Symbiotic Stars. I. Orbits for Well-Known S-Type Systems

Francis C. Fekel
Tennessee State University

Richard Joyce
National Optical Astronomy Observatory

Kenneth H. Hinkle
National Optical Astronomy Observatory

Michael F. Skrutskie
University of Massachusetts Amherst

THE ASTRONOMICAL JOURNAL, 119:1375–1388, 2000 March

INFRARED SPECTROSCOPY OF SYMBIOTIC STARS. I. ORBITS FOR WELL-KNOWN S-TYPE SYSTEMS

FRANCIS C. FEKEL[1]
Center of Excellence in Information Systems, Tennessee State University, 330 Tenth Avenue North, Nashville, TN 37203-3401; fekel@coe.tnstate.edu
RICHARD R. JOYCE AND KENNETH H. HINKLE
Kitt Peak National Observatory, National Optical Astronomy Observatories, P.O. Box 26732, Tucson, AZ 85726-6732; joyce@noao.edu, hinkle@noao.edu
AND
MICHAEL F. SKRUTSKIE
Department of Physics and Astronomy, University of Massachusetts, 517G Lederle Graduate Research Tower, Amherst, MA 01003-4525; skrutski@phast.umass.edu
Received 1999 September 13; accepted 1999 November 18

ABSTRACT

First results are reported for a program of monitoring symbiotic-star velocities in the 1.6 μm region with infrared-array technology. Infrared radial velocities have been used to determine single-lined spectroscopic orbits for six well-known symbiotic stars, EG And, T CrB, CI Cyg, BX Mon, RS Oph, and AG Peg. The new orbits are in general agreement with previous orbits derived from optical velocities. From the combined optical and infrared velocities improved orbital elements for the six systems have been determined. Each of the orbital periods has been determined solely from the radial-velocity data. With the addition of our new velocities, the orbital period of BX Mon has been revised to 1259 days, a 10% decrease from the previously reported result.

Key words: binaries: symbiotic — infrared radiation — stars: individual (AG Pegasi, BX Monocerotis, CI Cygni, EG Andromedae, RS Ophiuchi, T Coronae Borealis) — stars: late-type

1. INTRODUCTION

The class of symbiotic stars was identified by Merrill (1958) to include peculiar objects with spectra showing a cool giant-star continuum and absorption features combined with high-temperature emission lines. However, individual objects of the symbiotic type had been recognized long before. For instance, the peculiar spectrum of Z And was described 30 years prior by Plaskett (1928). For many decades, the nature of symbiotic stars was uncertain. Berman (1932) and Hogg (1934) suggested that the peculiar combination spectra of the stars now called *symbiotics* could be explained by a binary star. Unfortunately, at blue wavelengths, measuring accurate radial velocities of the cool absorption features to confirm the binary model is a daunting task. In that wavelength region, the spectrum of the cool giant is strongly contaminated by light from a circumstellar nebula and/or from a hot companion. Despite such problems, by the 1970s plausible orbits had been determined for several systems.

Two major advances have provided confirmation of the binary-star model. First, the launch of the *International Ultraviolet Explorer* (*IUE*) satellite enabled ultraviolet spectra of symbiotic stars to be obtained. Using such data, Kenyon & Webbink (1984) compared a range of binary models with the observed continua, which ranged from ultraviolet to infrared wavelengths, of about 20 symbiotic stars. They concluded that in many of the systems the ultraviolet continuum was due to a hot stellar source of roughly 80,000 K, while in others the hot component was associated with a probable main-sequence accretor. Using additional *IUE* spectra of symbiotic stars, Mürset et al. (1991) adapted the Zanstra method to determine the temperatures and luminosities of the hot components. They concluded that some of the hot components were white dwarfs, while others were similar to the central stars in planetary nebulae. Although these two groups did not always agree on the exact nature of the hot secondary in each symbiotic, nevertheless, their results demonstrated that the symbiotic stars are binaries. A second major advance was the measurement of radial velocities at 5200 Å, where the absorption-line spectrum of the cool giant begins to dominate the flux of the hot component (Garcia 1986). Over the next decade or so, Garcia, Kenyon, and collaborators used such observations to determine orbits for the cool component of at least 10 systems (e.g., Kenyon & Garcia 1986; Kenyon & Mikolajewska 1995). As a result of the ultraviolet and radial-velocity observations obtained over the past two decades, the binary nature of symbiotic stars is generally accepted. Indeed, Iben & Tutukov (1996) concluded that there is only one physical characteristic common to all symbiotic stars: they are all binaries.

A general view of the symbiotic class is that of mass-transfer systems with three spectroscopically detectable components. A cool giant or supergiant of spectral class K–M is the mass donor. If this giant has Mira-type variability, the system usually has a large infrared excess (see, e.g., Kenyon 1988). Such systems are the dusty or D-type symbiotic stars, while the nondusty systems are labeled as S type (Webster & Allen 1975). A circumstellar ionized nebula is present with an electron temperature $\sim$17,000 K. The nature of the mass-accreting secondary divides the symbiotic stars into two physically distinct subclasses. In most symbiotic stars, the secondary is a degenerate star, typically a white dwarf with an effective temperature $\sim$100,000 K. In one case, that of V2116 Oph, the secondary is a neutron star (Chakrabarty & Roche 1997). The accretion rate onto the degenerate star is 10^{-9}–10^{-7} $M_\odot$ yr^{-1} as the result of captured wind from the giant. Symbiotic stars belonging to

[1] Visiting Astronomer, Kitt Peak National Observatory, National Optical Astronomy Observatories, which are operated by the Association of Universities for Research in Astronomy, Inc., under cooperative agreement with the National Science Foundation.

the other subclass, a much less numerous group (Kenyon 1986), are thought to have a main-sequence star as a secondary. Such systems have Roche-lobe–filling primaries and significantly higher ($\gtrsim 10^{-5}$ $M_\odot$ yr^{-1}) mass-transfer rates (Iben & Tutukov 1996). Recently, Mürset & Schmid (1999) stated that as a result of new observations, the number of symbiotic stars believed to be in this latter subclass has decreased.

While absorption features at yellow and longer wavelengths are now being used to produce good orbits for the cool giants, the orbits of the hot components are more difficult to determine. In the best cases, velocities of emission features presumed to be associated with the hot component have been measured, and the mass ratios of the stars have been computed. Then, various assumptions have been used to estimate the masses, radii, and separation of the components, as well as the Roche-lobe radius of the cool giant. Such basic data leads to a determination of whether or not these mass-exchange systems are detached or whether the giants fill their Roche lobes (e.g., Seal 1997). In addition, the orbital eccentricity provides information on the evolution of the system.

Although orbital elements are critical for an understanding of these systems, only about a dozen of the ~ 150 known symbiotic stars currently have reasonably well-determined orbits for the cool giant (Seal 1997). This lack of information is a measure of the difficulty of determining even single-lined orbits for symbiotic stars. In addition to previously mentioned problems associated with velocity measurement at blue wavelengths, symbiotic stars have orbital periods ranging from about 6 months to ~ 100 yr (Whitelock 1987) and low velocity amplitudes. Thus, determining accurate orbital parameters has been neither a quick nor easy process.

Our interest in symbiotic systems stems from the realization that attempts to observe the cool star in the visual are hampered by both the emission-line spectrum and scattering by dust, if present, from the cool star. The 1–2 μm region of the infrared offers a window with much-reduced dust extinction that is nearly free from contamination by the hot star. In addition, the D-type symbiotic stars contain Mira variables, and infrared spectroscopy of Mira variables (see, e.g., Hinkle, Lebzelter, & Scharlach 1997) clearly demonstrates the benefits of observing these stars near the H^- opacity minimum at 1.6 μm; spectra of Mira variables in the 1–2 μm infrared show cyclically repeatable, large-amplitude (20–30 km s^{-1}) velocity changes during a pulsation period. With a few exceptions this cannot be observed in the visual.

This paper extends our work on the orbits of symbiotic stars obtained from infrared data (Hinkle et al. 1989, 1993). Previous results were based on spectra obtained at the Kitt Peak National Observatory (KPNO) 4 m Mayall Telescope with a Fourier transform spectrometer (FTS). The FTS provided spectra of remarkable accuracy and large bandwidth, but those same characteristics limited the FTS to the brightest infrared stars. With the advent of sensitive infrared arrays, we have expanded our symbiotic-star program to include about two dozen northern symbiotic stars by using an infrared array in combination with a warm spectrograph. High-resolution spectra of all the known galactic symbiotic stars could be easily observed by cryogenic infrared spectrographs (Hinkle et al. 1998) on large telescopes, but long-term monitoring projects are much more easily carried out on small telescopes with inexpensive equipment. This paper is a demonstration of our technique. We determine single-lined spectroscopic orbits for the cool giant of six S-type symbiotic stars and compare our results with previously published orbits. The basic data for these stars are given in Table 1. In future papers, we will discuss observations of D-type symbiotic stars as well as orbits for additional S-type systems, including some whose orbits will be determined for the first time.

2. OBSERVATIONS AND REDUCTIONS

Most of our spectroscopic observations of the six program stars were obtained with the 0.9 m coudé feed telescope and spectrograph system at KPNO. We employed the NICMASS camera and a 256 × 256 HgCdTe imager developed at the University of Massachusetts, at the focus of camera 5 in the same location normally occupied by an optical CCD detector. With the 31.6 line mm^{-1} echelle grating, we obtained a 2 pixel resolving power of 44,000, quite sufficient for obtaining radial velocities to a precision better than 1 km s^{-1}. A more complete description of the experimental setup may be found in Joyce et al. (1998).

The ambient temperature of the spectrograph room produces significant thermal background even at a wavelength of 1.6 μm. We were able to reduce this significantly by installing a narrowband (1% FWHM) filter centered at 1.623 μm inside the NICMASS cryostat. The spectral coverage defined by the array ($\sim 0.3\%$) fits well within the filter bandpass. The free spectral range of the echelle order used

TABLE 1

BASIC PROPERTIES OF PROGRAM STARS

Name	HR/HD	V[a] (mag)	K[b] (mag)	$H-K$[b] (mag)	Primary Spectral Type[c]	Orbital Period (days)	$\dot{M}$[d] ($M_\odot$ yr^{-1})
EG And	HD 4174	7.1–7.8	2.6	0.20	M3 III	483	9×10^{-9}
T CrB[e].....	HR 5958	2.0–10.8	4.7	0.25	M4.5 III	228	$< 2 \times 10^{-8}$
CI Cyg	...	9.9–13.1	4.5	0.31	M5.5 II	854	3×10^{-7}
BX Mon.....	...	9.5–13.4	5.7	0.28	M5 III	1259	$< 5 \times 10^{-8}$
RS Oph[f].....	HD 162214	4.3–12.5	6.6	0.33	K7 I–II	456	$< 6 \times 10^{-8}$
AG Peg	HD 207757	6.0–9.4	3.9	0.24	M3 III	818	8×10^{-8}

[a] From Kholopov 1985.
[b] From Kenyon 1988. BX Mon and RS Oph are slightly variable (approximately ± 0.1 mag) at K.
[c] Temperature classes are from Mürset & Schmid 1999; luminosity classes are from Kenyon & Fernández-Castro 1987.
[d] From Seaquist, Krogulec, & Taylor 1993.
[e] T CrB was Nova CrB 1866 and 1946. $V = 2.0$ is the Nova brightness.
[f] RS Oph was Nova Oph 1898, 1933, and 1967.

(35th order) is much larger than the filter bandwidth. This spectral region is ideal for this project as it contains a number of lines in the 6–3 CO band and is essentially free of telluric absorption lines. Even with the narrowband filter, the sensitivity of our observations was limited by the thermal background, which gave a signal of 20–80 electrons s^{-1}, depending on the temperature of the spectrograph room. This was still sufficiently small to permit exposure times of 60 minutes for the fainter program objects.

Because of the large background on the array, observations were taken in pairs; the object was placed on the slit at two positions separated by approximately 20 pixels. The two observations of each object were subtracted to remove the background, flat-fielded, and extracted in the usual manner with the IRAF task APEXTRACT. This is a standard technique (cf. Joyce 1992) for the reduction of infrared spectra.

Wavelength calibration posed a challenge, because the spectral coverage was far too small to include a sufficient number of ThAr emission lines for a dispersion solution. Our approach was to utilize the CO lines in a K III star to obtain a dispersion solution and correct for the zero offset with the two telluric 4–2 $P_{1e/f}(4.5)$ OH emission lines in the raw data. Those sky lines provide a precise wavelength standard and require no assumptions about the radial velocity of the calibration star. Representative spectra are shown in Figure 1.

On three nights observations were obtained with the Phoenix Spectrograph at the f/15 Cassegrain focus of either the KPNO 2.1 or 4 m telescope. Phoenix is a cryogenic, echelle spectrograph employing a 31.6 line mm^{-1} grating and a 512 × 1024 InSb array. In all cases the widest slit was used, giving a resolution ~40,000. A complete description of the spectrograph can be found in Hinkle et al. (1998). As with the NICMASS observations, a narrowband blocking filter was used. The Phoenix observations were centered at 1.563 μm, a spectral region totally free of telluric absorption lines that is dominated by 3–0 CO lines in cool stars. While there is little contribution from thermal background at this wavelength when observing with Phoenix, spectra were observed in pairs to cancel instrumental and detector effects. As with the NICMASS spectra, the dispersion solution was obtained from CO lines in a reference-star spectrum and the zero offset measured from OH emission lines, in this case 3–1 $P_{1e/f}(6.5)$ and 3–1 $P_{2e/f}(5.5)$, in the raw data. Representative spectra are shown in Figure 2.

Radial velocities of the program stars were determined with the IRAF cross-correlation program FXCOR (Fitzpatrick 1993). The velocities are referenced to observations of M-giant IAU velocity standards, δ Oph or α Cet, which were obtained multiple times during the course of each night. The radial velocities of the standard stars were adopted from the work of Scarfe, Batten, & Fletcher (1990).

Several different computer programs, used to determine the orbital elements of the various systems, are mentioned in the individual orbital-elements sections. Preliminary elements often were determined with BISP, a computer program that uses a slightly modified version of the Wilsing-Russell method (Wolfe, Horak, & Storer 1967). A differential-corrections program, called SB1, of Barker,

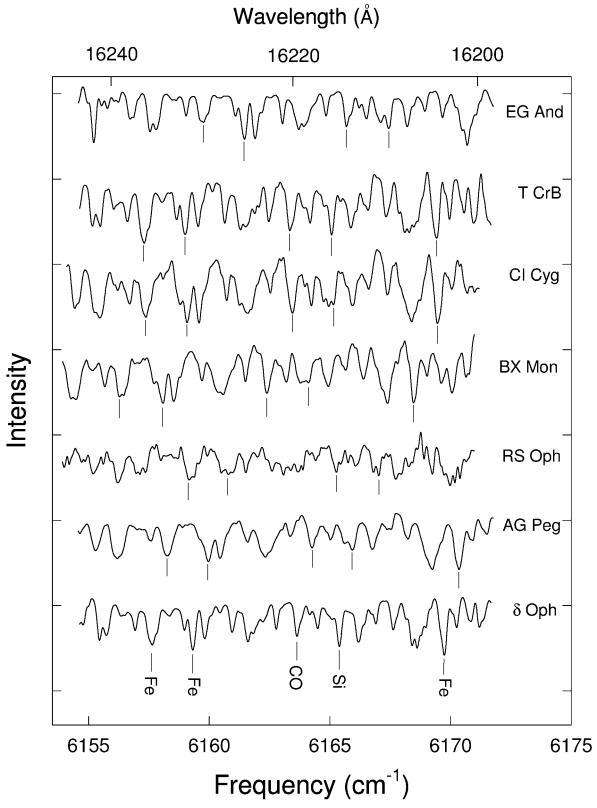

FIG. 1.—Representative spectra of the six program stars and the velocity standard δ Oph (M0.5 III) obtained with the NICMASS dewar at the coudé feed spectrograph. Each spectrum is successively offset by 1.0 in relative intensity. The UT dates of the symbiotic-star observations are as follows: AG Peg, 1999 June 18; CI Cyg, 1999 May 5; EG And, 1999 June 18; RS Oph, 1999 April 26; T CrB, 1999 June 16; BX Mon, 1999 April 26. The reference star (δ Oph) was observed on 1999 June 16.

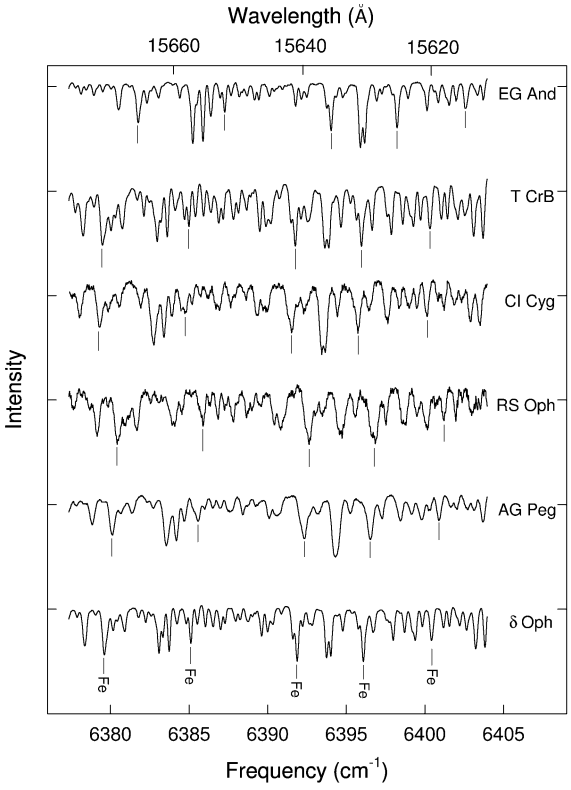

FIG. 2.—Representative spectra of five program stars and the velocity standard δ Oph (M0.5 III) obtained with the cryogenic Phoenix Spectrograph. Each spectrum is successively offset by 1.0 in relative intensity. All spectra in this figure were obtained on 1999 July 4 UT except for that of CI Cyg, which was obtained on 1999 July 3 UT.

Evans, & Laing (1967) has been used to compute eccentric orbits of single-lined systems. For most systems the orbital eccentricity is small enough that a circular-orbit solution may be appropriate. In those cases such an orbit was computed with SB1C (D. Barlow 1998, private communication), which also uses differential corrections to determine the orbital elements. As recommended by Batten, Fletcher, & MacCarthy (1989), for circular orbits we have identified T_0 as a time of maximum velocity.

Velocity sets from other observatories were included in the final orbital solutions. For a given set of velocities, if the phase distribution was relatively uniform and the number of velocities large enough, an independent orbit was computed and compared with a similar orbit computed with our velocities alone. The weights of the individual velocities in each data set were determined from the ratio of the variance of the velocities for the two solutions.

3. EG ANDROMEDAE

3.1. *Brief Orbital History*

Smith (1980) analyzed variations in the radial velocity and equivalent width of Hα, from which he determined a period of 470 days for the M giant. Oliversen et al. (1985) measured the velocities of absorption lines in the Hα region and, assuming Smith's (1980) period, determined a preliminary orbit from their eight velocities. From 1966 to 1987, Skopal et al. (1991) obtained 44 spectra, mostly at blue wavelengths. With their measured absorption-line radial velocities and additional velocities in the literature, Skopal et al. (1991) determined a period of 482 days and an eccentricity of 0.29 ± 0.07. Munari et al. (1988) and Munari (1993) obtained velocities at yellow and red wavelengths. Munari (1993) used those two sets of velocities, combined with previously published ones, to produce an orbit with a period of 481.1 days and an eccentricity of 0.14 ± 0.08. Wilson & Vaccaro (1997) analyzed B and V light curves of EG And. They argued that the sinusoidal light variations are the result of tidal distortion, the ellipsoidal effect. From a reanalysis of selected radial-velocity data sets and their best-fit light curve, they concluded that the orbit is likely circular. The most reliable orbital elements currently available appear to be those of Kenyon (1992), who obtained absorption-line velocities in the 5200 Å region. His orbit is essentially circular and has a period of 480.7 days, but most of the velocities for that orbit are unpublished.

3.2. *Orbital Elements*

From 1996 October to 1999 July, we obtained 10 radial velocities of EG And (see Table 2). Assuming a period of 482 days (Skopal 1997), we computed preliminary orbital elements with BISP and refined them with SB1. Our elements, shown in Table 3, are in excellent agreement with those of Kenyon (1992). Since our eccentricity is quite low, 0.045 ± 0.026, a circular-orbit solution was computed with SB1C. The precepts of Lucy & Sweeney (1971) indicate that a circular orbit is to be preferred for our velocities.

To determine a final orbit, we have analyzed our velocities plus the eight velocities from Oliversen et al. (1985), 15 from Munari et al. (1988; the velocity of JD 2,446,894 was excluded because of its very large residual), and 13 from Munari (1993). Other radial velocities exist but are of lower quality, are very few in number, or have not been published. First, a circular orbit was determined separately for each of the three data sets from the literature. When compared with the circular orbit for our KPNO velocities, no zero-point velocity correction was applied to any of the three sets of observations. From a comparison of the variance of the velocities for each solution, the velocities in the three data sets were given weights of 0.07, 0.03, and 0.20, respectively, relative to our velocities. Then, both eccentric- and circular-orbit solutions were computed with the 46 velocities.

For several reasons we have chosen to list the circular-orbit solution as the final one. Although the criteria of Lucy & Sweeney (1971) indicate that an eccentric-orbit solution is to be preferred, the results are close to the dividing lines of both tests. The eccentricity of our all-data solution is

TABLE 2

RADIAL VELOCITIES OF EG ANDROMEDAE

HJD (2,400,000+)	Phase	Velocity (km s^{-1})	$O-C$ (km s^{-1})	Weight	Source[a]
44,100.100.....	0.108	−88.3	1.0	0.07	O85
44,246.600.....	0.412	−100.2	1.0	0.07	O85
44,420.900.....	0.773	−94.5	−0.6	0.07	O85
44,650.500.....	0.249	−94.6	0.3	0.07	O85
44,856.900.....	0.677	−98.3	0.0	0.07	O85
44,915.800.....	0.799	−91.2	1.6	0.07	O85
44,921.800.....	0.811	−88.2	4.1	0.07	O85
45,193.900.....	0.375	−103.4	−3.2	0.07	O85
45,660.000.....	0.341	−103.0	−4.0	0.03	M88
45,714.000.....	0.453	−103.0	−1.0	0.03	M88
46,048.000.....	0.145	−89.0	1.5	0.03	M88
46,344.000.....	0.758	−95.0	−0.4	0.03	M88
46,372.000.....	0.816	−90.0	2.0	0.03	M88
46,372.000.....	0.816	−91.0	1.0	0.03	M88
46,688.000.....	0.471	−101.0	1.2	0.03	M88
46,693.000.....	0.481	−100.0	2.3	0.03	M88
46,693.000.....	0.481	−101.0	1.3	0.03	M88
46,745.000.....	0.589	−103.0	−1.8	0.03	M88
46,752.000.....	0.604	−103.0	−2.2	0.03	M88
46,753.000.....	0.606	−101.0	−0.2	0.20	M93
46,753.000.....	0.606	−98.0	2.8	0.20	M93
46,763.000.....	0.626	−97.0	3.1	0.03	M88
46,764.000.....	0.629	−99.0	1.1	0.03	M88
46,784.000.....	0.670	−104.0	−5.5	0.03	M88
46,819.000.....	0.742	−100.0	−4.7	0.03	M88
46,925.000.....	0.962	−87.0	0.9	0.20	M93
47,015.000.....	0.149	−90.0	0.6	0.20	M93
47,017.000.....	0.153	−91.0	−0.2	0.20	M93
47,104.000.....	0.333	−98.0	0.6	0.20	M93
47,164.000.....	0.457	−100.0	2.1	0.20	M93
47,197.000.....	0.526	−99.0	3.2	0.20	M93
47,223.000.....	0.580	−100.0	1.4	0.20	M93
47,312.000.....	0.764	−96.0	−1.6	0.20	M93
47,314.000.....	0.768	−94.0	0.2	0.20	M93
47,315.000.....	0.770	−95.0	−0.9	0.20	M93
47,344.000.....	0.830	−92.0	−0.5	0.20	M93
50,386.867.....	0.136	−90.4	−0.2	1.00	KPNO
50,629.992.....	0.640	−100.1	−0.4	1.00	KPNO
50,688.991.....	0.762	−94.9	−0.5	1.00	KPNO
50,750.837.....	0.890	−89.7	−0.3	1.00	KPNO
50,935.015.....	0.272	−96.7	−0.7	1.00	KPNO
50,982.980.....	0.371	−100.8	−0.7	1.00	KPNO
51,106.909.....	0.628	−100.4	−0.3	1.00	KPNO
51,135.818.....	0.688	−97.2	0.6	1.00	KPNO
51,347.970.....	0.128	−89.5	0.4	1.00	KPNO
51,363.885.....	0.161	−90.6	0.5	1.00	KPNO

[a] (O85) Oliversen et al. 1985; (M88) Munari et al. 1988; (M93) Munari 1993; (KPNO) this paper.

TABLE 3

ORBITAL ELEMENTS OF EG ANDROMEDAE

Parameter	Kenyon 1992	KPNO-Data Solution	Final Solution
P (days).....	480.7	482.0 (fixed)	482.57 ± 0.53
T (HJD).....	...	$2{,}451{,}422 \pm 82$	...
T_0[a] (HJD).....	...	...	$2{,}450{,}803.8 \pm 2.3$
γ (km s^{-1}).....	-95.0	-95.3 ± 0.2	-95.00 ± 0.16
K_1 (km s^{-1}).....	7.5	7.7 ± 0.3	7.32 ± 0.27
e.....	0.043 ± 0.021	0.04 ± 0.03	0.0
ω_1 (deg).....	...	102 ± 61	...
$a_1 \sin i$ (km).....	...	$51 \pm 2 \times 10^6$	$48.6 \pm 1.8 \times 10^6$
$f(m)$[b].....	0.021	0.022 ± 0.002	0.0196 ± 0.0022

[a] T_0 is the time of maximum velocity.
[b] $f(m) = (m_2)^3 \sin^3 i/(m_1 + m_2)^2$.

0.101 ± 0.041, somewhat larger than the value of 0.045 ± 0.026 from our data alone, which have the highest weights. This latter value is essentially identical with Kenyon's (1992) small eccentricity. Finally, the assumption of a circular orbit is consistent with the findings of Wilson & Vaccaro (1997).

The individual velocities and their residuals to the all-data circular orbit are given in Table 2, and the final orbital elements are listed in Table 3. Since the orbit is assumed to be circular, a time of maximum velocity, T_0, is listed rather than T, a time of periastron passage. Figure 3 compares the radial velocities with the computed velocity curve, where zero phase is computed from T_0.

4. T CORONAE BOREALIS

4.1. *Brief Orbital History*

Major progress in understanding the nature of the recurrent nova T CrB occurred when Sanford (1949) discovered that the M giant underwent velocity variations with a period of 230.5 days and had a semiamplitude of 21 km s^{-1}. Kraft (1958) obtained seven new spectroscopic observations. Combining his velocities with those of Sanford (1949) and a few earlier velocities, Kraft (1958) determined a double-lined orbit and revised the period to 227.6 days. With telescopes of the Smithsonian Astrophysical Observatory (SAO), Kenyon & Garcia (1986) obtained 25 additional velocities from a 44 Å bandpass centered near 5200 Å. Independent solutions of their data and the combined data of Kraft (1958) and Sanford (1949) resulted in similar orbital elements. Thus, Kenyon & Garcia (1986) produced a final circular-orbit solution of all those M-giant velocities.

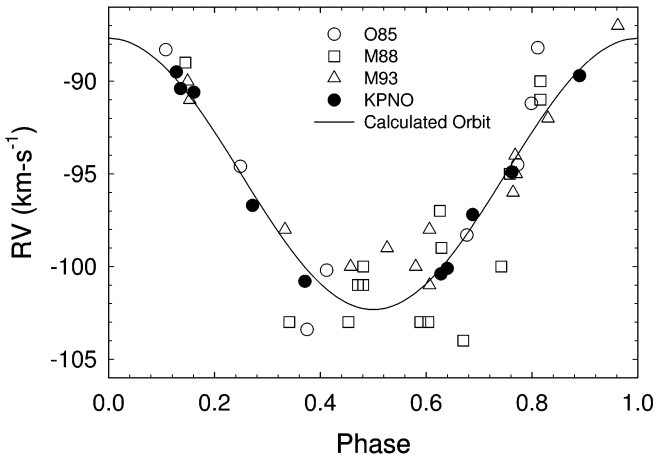

FIG. 3.—Computed radial-velocity curve of EG And compared with the observed velocities. Zero phase is a time of maximum velocity.

For the hot component, Kraft (1958) measured velocities of the Hβ emission lines, resulting in a mass ratio of 1.4, with the M giant being the more massive object. Recently, Belczyński & Mikolajewska (1998) have proposed that the M giant is less massive than its companion. Using several lines of argument, they assumed that the hotter object is a massive white dwarf and showed that in that case, the M giant is the much less massive object.

4.2. *Orbital Elements*

From 1997 April to 1999 July, we obtained nine velocities of T CrB (see Table 4). Assuming a period of 227.53 days from the all-data solution of Kenyon & Garcia (1986), preliminary elements of our velocities were determined with BISP and refined with SB1. The eccentricity of the latter solution is quite small, 0.008 ± 0.012, and is consistent with the orbit being circular. Thus, such an orbit, computed from our data with SB1C, is compared in Table 5 with the all-data solution of Kenyon & Garcia (1986). The two center-of-mass velocities are in excellent agreement, and our semiamplitude is only 5% larger than that found by Kenyon & Garcia (1986). As a result, a new combined solution has been computed that includes the velocities used by Kenyon & Garcia (1986) as well as our velocities.

To determine the velocity offsets and the weights of the velocities in the various data sets, we computed a circular orbit of the SAO data using the elements of Kenyon & Garcia (1986). A comparison of the velocity variances for the circular orbit of the KPNO data with that of the SAO solution indicated weights of 0.2 for the individual SAO velocities. A similar comparison of our KPNO solution with a circular orbit for Sanford's (1949) 20 velocities resulted in weights of 0.02 and a zero-point velocity shift of -1.4 km s^{-1} for those velocities. We note that Sanford's (1949) velocity of 1948 May, which was based on only five lines, had a 3 σ residual and was rejected from the solution. Finally, from a circular-orbit solution for the seven velocities of Kraft (1958), weights of 0.3 were assigned to those velocities.

With the above 60 velocities appropriately weighted, we computed eccentric- and circular-orbit solutions using SB1 and SB1C. Following the precepts of Lucy & Sweeney (1971), a circular orbit is clearly to be preferred, and it is listed in Table 5. The velocities and velocity residuals to our final orbit are given in Table 4. Figure 4 compares the

TABLE 4

RADIAL VELOCITIES OF T CORONAE BOREALIS

HJD (2,400,000+)	Phase	Velocity (km s^{-1})	$O-C$ (km s^{-1})	Weight	Source[a]
31,895.964.....	0.592	−44.2	3.6	0.02	S49
31,925.872.....	0.723	−32.4	−0.6	0.02	S49
31,954.885.....	0.851	−20.0	−6.4	0.02	S49
31,957.785.....	0.864	−10.4	1.7	0.02	S49
32,070.688.....	0.360	−44.0	−1.0	0.02	S49
32,195.042.....	0.906	−11.6	−3.7	0.02	S49
32,196.007.....	0.910	−6.2	1.4	0.02	S49
32,224.976.....	0.038	−3.4	1.2	0.02	S49
32,256.957.....	0.178	−16.8	0.6	0.02	S49
32,258.946.....	0.187	−16.6	2.0	0.02	S49
32,275.826.....	0.261	−34.0	−4.5	0.02	S49
32,305.969.....	0.394	−40.7	5.8	0.02	S49
32,308.825.....	0.406	−48.5	−0.9	0.02	S49
32,343.757.....	0.560	−49.0	1.0	0.02	S49
32,370.803.....	0.679	−36.4	1.7	0.02	S49
32,404.719.....	0.828	−14.6	2.0	0.02	S49
32,600.976.....	0.690	−40.2	−3.6	0.02	S49
32,669.787.....	0.992	−10.3	−6.4	0.02	S49
32,695.887.....	0.107	−9.3	−0.2	0.02	S49
35,583.800.....	0.797	−21.2	−0.4	0.30	K58
35,617.700.....	0.946	−5.0	0.2	0.30	K58
35,647.800.....	0.079	−7.4	−0.6	0.30	K58
35,671.800.....	0.184	−17.4	0.8	0.30	K58
35,675.700.....	0.201	−20.5	0.1	0.30	K58
35,938.700.....	0.357	−43.2	−0.6	0.30	K58
35,993.800.....	0.599	−45.9	1.3	0.30	K58
45,037.024.....	0.337	−39.6	0.7	0.20	KG86
45,064.963.....	0.460	−50.9	0.0	0.20	KG86
45,071.866.....	0.491	−51.3	0.3	0.20	KG86
45,097.858.....	0.605	−45.9	0.8	0.20	KG86
45,152.731.....	0.846	−13.3	0.9	0.20	KG86
45,243.604.....	0.245	−25.8	1.3	0.20	KG86
45,368.055.....	0.792	−23.2	−1.7	0.20	KG86
45,426.838.....	0.050	−5.9	−0.8	0.20	KG86
45,426.851.....	0.050	−5.9	−0.8	0.20	KG86
45,426.863.....	0.051	−5.9	−0.8	0.20	KG86
45,426.878.....	0.051	−5.8	−0.7	0.20	KG86
45,449.867.....	0.152	−15.7	−1.8	0.20	KG86
45,508.626.....	0.410	−47.3	0.6	0.20	KG86
45,508.709.....	0.410	−47.1	0.9	0.20	KG86
45,718.008.....	0.330	−39.5	−0.2	0.20	KG86
45,818.766.....	0.773	−23.4	1.0	0.20	KG86
45,835.704.....	0.847	−12.7	1.4	0.20	KG86
45,866.600.....	0.983	−3.0	1.0	0.20	KG86
45,871.659.....	0.005	−2.7	1.2	0.20	KG86
45,895.571.....	0.110	−8.8	0.6	0.20	KG86
45,963.508.....	0.409	−48.6	−0.8	0.20	KG86
46,075.972.....	0.903	−10.4	−2.2	0.20	KG86
46,093.898.....	0.982	−5.0	−0.9	0.20	KG86
46,133.898.....	0.157	−16.4	−1.7	0.20	KG86
46,140.814.....	0.188	−19.0	−0.3	0.20	KG86
50,568.762.....	0.645	−42.6	−0.2	1.00	KPNO
50,627.706.....	0.904	−7.3	0.8	1.00	KPNO
50,932.932.....	0.246	−27.1	0.0	1.00	KPNO
50,981.747.....	0.460	−51.7	−0.8	1.00	KPNO
51,107.579.....	0.013	−4.3	−0.3	1.00	KPNO
51,294.829.....	0.836	−15.8	−0.3	1.00	KPNO
51,345.712.....	0.060	−5.5	0.1	1.00	KPNO
51,362.731.....	0.134	−11.4	0.5	1.00	KPNO
51,363.672.....	0.139	−12.5	−0.1	1.00	KPNO

[a] (S49) Sanford 1949; (K58) Kraft 1958; (KG86) Kenyon & Garcia 1986; (KPNO) this paper.

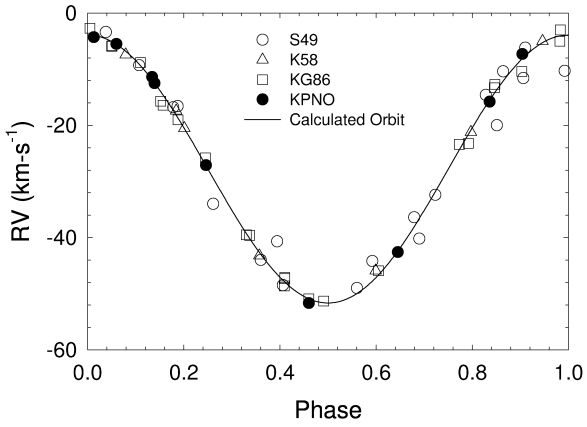

FIG. 4.—Same as Fig. 3, but for T CrB

velocities with the computed velocity curve, where zero phase is computed from T_0, a time of maximum velocity.

5. CI CYGNI

5.1. *Brief Orbital History*

Using visual and photographic observations, Whitney (see Aller 1954) determined a period of 855.25 days for the photometric variability of CI Cyg. Belyakina (1979, 1984) confirmed this period and concluded that the star is an eclipsing binary. The best orbital elements of the M giant are those of Kenyon et al. (1991), who used the cross-correlation technique to measure absorption-line radial velocities in the 5200 Å region. From their 41 velocities, which cover three orbital cycles, they found a period of 844 ± 34 days, consistent with the photometric period of 855.25 days. As a result, they adopted the photometric period for their orbital solutions. They computed both a circular and an eccentric orbit for the cool star and favored the latter, which had an eccentricity of 0.15 ± 0.08. Kenyon et al. (1991) examined several emission lines to see whether they followed the orbital motion of the hot component. They found that the best tracer of the hot component's motion is the He II line at 4686 Å. Their resulting mass ratio for the cool giant to the hot component is 3.1 ± 0.5.

5.2. *Orbital Elements*

From 1997 June to 1999 July, we obtained 9 radial velocities of CI Cyg (see Table 6). Using a period of 855.25 days, which was also assumed by Kenyon et al. (1991), we computed preliminary orbital elements with BISP and refined them with SB1. Our eccentric-orbit solution and that of Kenyon et al. (1991) have eccentricities of 0.1–0.15, but both values have large errors.

Circular orbits for each of the two data sets were computed with SB1C. According to the precepts of Lucy & Sweeney (1971), a circular orbit is to be preferred in each case. Table 7 compares the elements of our circular orbit with those of Kenyon et al. (1991). The semiamplitudes are in excellent agreement, while the center-of-mass velocities differ by 3.2 km s^{-1}. That amount was added to each of the Kenyon et al. (1991) velocities, and from a comparison of the variances of the two sets of velocities, the SAO velocities were given weights of 0.2 relative to the KPNO velocities.

With the 51 velocities, which cover seven orbital cycles, and the period as a free parameter, we determined both circular- and eccentric-orbit solutions. Following from

TABLE 5

ORBITAL ELEMENTS OF T CORONAE BOREALIS

Parameter	Kenyon & Garcia 1986	KPNO-Data Solution	Final Solution
P (days).....	227.53 ± 0.02	227.53 (fixed)	227.5687 ± 0.0099
T_0 (HJD)	2,431,990.71 ± 0.13	2,451,104.6 ± 0.3	2,447,918.62 ± 0.27
γ (km s^{-1}).....	−27.89 ± 0.06	−27.9 ± 0.2	−27.79 ± 0.13
K_1 (km s^{-1}).....	23.32 ± 0.16	24.2 ± 0.2	23.89 ± 0.17
e	0.0	0.0	0.0
ω_1 (deg)	...	...	...
$a_1 \sin i$ (km)	73.0 ± 0.6 × 10^6	75.9 ± 0.7 × 10^6	74.77 ± 0.53 × 10^6
$f(m)$	0.299 ± 0.006	0.34 ± 0.01	0.3224±0.0068

Lucy & Sweeney (1971), it is not clear which solution is preferred. The similar eccentricities found in the separate solutions of the Kenyon et al. (1991) data and our KPNO data apparently are reinforced enough in the combined solution to make the eccentric orbit viable. Thus, that final solution has been listed in Table 7 with velocities and residuals to that solution given in Table 6. Figure 5 compares the radial velocities with the computed velocity curve. Zero phase is a time of periastron passage.

As can be seen in Figure 5, the velocities, particularly those of Kenyon et al. (1991), are not uniformly distributed in phase and may bias the orbital solution toward one with a nonzero eccentricity. However, the assumption of a circular or eccentric orbit is not critical since within the uncertainties the values of the periods, semiamplitudes, and mass functions of our final circular and eccentric solutions are the same. Our spectroscopically determined period of 853.8 days (Table 7) is in excellent agreement with the photometric period of 855.25 days. In fact, Kenyon et al. (1991) stated that recent eclipses indicate that the photometric period should be 1–2 days shorter than the quoted value, which would bring the two period determinations into even closer accord.

6. BX MONOCEROTIS

6.1. *Brief Orbital History*

Mayall (1940) found a periodicity of 1380 days for the light variations of BX Mon, but Iijima's (1985) more recent spectroscopic observations were inconsistent with such a period. Despite that problem, Iijima (1985) proposed that BX Mon is a long-period eclipsing binary with an eccentric orbit. Dumm et al. (1998) reanalyzed the data from 1890 to 1940 used by Mayall (1940) and included visual-brightness estimates from 1989 to 1995, which were supplied by the Royal Astronomical Society of New Zealand (RASNZ). Analyzing the combined data, they found two possible periods, 1338 ± 8 days and 1401 ± 8 days. From the phase distribution of fluxes computed for several *IUE* spectra, they concluded that BX Mon is an eclipsing binary having a period of 1401 ± 8 days.

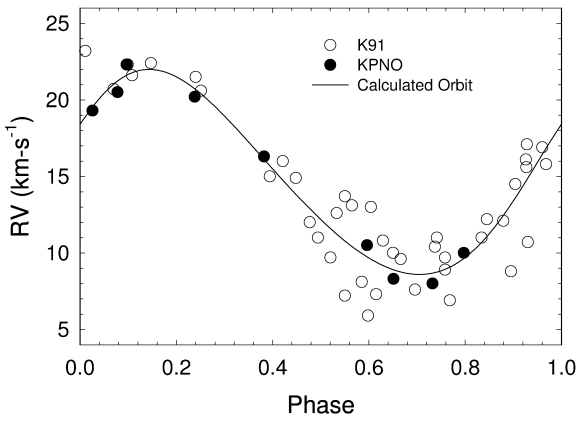

FIG. 5.—Computed radial-velocity curve of CI Cyg compared with the observed velocities. Zero phase is a time of periastron passage.

Dumm et al. (1998) obtained high-dispersion spectra at both blue and red wavelengths. Assuming a period of 1401 days, they computed an orbit for the M giant from 18 velocities measured at wavelengths between 6500 and 7500 Å. They found the system to have a high eccentricity of 0.49, confirming the suggestion of Iijima (1985).

Michalitsianos et al. (1982) obtained low-dispersion ultraviolet spectra with the *IUE* satellite and found that both absorption features and a continuum characteristic of a late A- or early F-type hot component are visible. Dumm et al. (1998) noted that spectra covering wavelengths blueward of 6000 Å showed evidence of a hot companion, and they were able to measure absorption features of that component in two blue-wavelength spectra. They determined the mass ratio of the cool-to-hot components to be 6.7 ± 1.3 and suggested that the hot component is a white dwarf.

6.2. *Orbital Elements*

From 1995 October to 1999 April, we obtained 11 velocities of BX Mon (see Table 8). Assuming the orbital period of Dumm et al. (1998) and using the rest of their elements as starting values, we computed orbital elements of the M giant with the SB1 program. Since those elements appeared to be in reasonable agreement with those of Dumm et al. (1998), we analyzed together our velocities and the 17 velocities of Dumm et al. (1998). Our observations began just before those of Dumm et al. (1998) ended, and so, one additional orbital cycle has been observed now. A period search of the 28 velocities identified a single best period of 1262 ± 32 days, which differs by 10% from the value of 1401 days.

Figure 1*c* of Dumm et al. (1998) is a plot of the RASNZ 1989–1995 visual observations of BX Mon, which were phased with their 1401 days period. However, in that figure the observations at the epochs of "rapid" brightening do not appear to be aligned. A period analysis of the same RASNZ data resulted in a single best period of 1302 ± 25 days, in agreement with our radial-velocity period of 1262 ± 32 days. Those RASNZ visual observations plotted modulo the 1302 days period are shown in Figure 6, where zero phase is 2,449,796.03 (HJD), a time of conjunction with

TABLE 6

RADIAL VELOCITIES OF CI CYGNI

HJD (2,400,000+)	Phase	Velocity (km s^{-1})	$O-C$ (km s^{-1})	Weight	Source[a]
45,243.719.....	0.930	10.7	−4.2	0.2	K91
45,517.979.....	0.251	20.6	0.2	0.2	K91
45,662.562.....	0.421	16.0	1.2	0.2	K91
45,785.994.....	0.565	13.1	2.7	0.2	K91
45,818.906.....	0.604	13.0	3.4	0.2	K91
45,840.866.....	0.629	10.8	1.6	0.2	K91
45,871.800.....	0.666	9.6	0.8	0.2	K91
45,950.750.....	0.758	9.7	0.8	0.2	K91
46,096.036.....	0.928	17.1	2.3	0.2	K91
46,249.777.....	0.108	21.6	−0.2	0.2	K91
46,282.684.....	0.147	22.4	0.4	0.2	K91
46,362.627.....	0.240	21.5	0.8	0.2	K91
46,564.828.....	0.477	12.0	−0.9	0.2	K91
46,600.916.....	0.520	9.7	−1.9	0.2	K91
46,626.707.....	0.550	7.2	−3.6	0.2	K91
46,656.692.....	0.585	8.1	−1.9	0.2	K91
46,682.772.....	0.615	7.3	−2.1	0.2	K91
46,712.595.....	0.650	10.0	1.1	0.2	K91
46,751.593.....	0.696	7.6	−1.0	0.2	K91
46,786.553.....	0.737	10.4	1.7	0.2	K91
46,804.540.....	0.758	8.9	0.0	0.2	K91
46,878.981.....	0.845	12.2	1.1	0.2	K91
46,907.940.....	0.879	12.1	−0.3	0.2	K91
46,928.906.....	0.904	14.5	0.9	0.2	K91
46,948.844.....	0.927	15.6	0.9	0.2	K91
46,983.709.....	0.968	15.8	−1.0	0.2	K91
47,020.721.....	0.011	23.2	4.3	0.2	K91
47,070.660.....	0.070	20.7	−0.3	0.2	K91
47,095.574.....	0.099	22.3	0.6	0.2	K91
47,347.776.....	0.394	15.0	−0.7	0.2	K91
47,393.708.....	0.448	14.9	1.1	0.2	K91
47,432.621.....	0.494	11.0	−1.4	0.2	K91
47,466.583.....	0.533	12.6	1.4	0.2	K91
47,480.567.....	0.550	13.7	2.9	0.2	K91
47,521.550.....	0.598	5.9	−3.8	0.2	K91
47,643.924.....	0.741	11.0	2.3	0.2	K91
47,666.976.....	0.768	6.9	−2.2	0.2	K91
47,722.889.....	0.834	11.0	0.3	0.2	K91
47,775.656.....	0.895	8.8	−4.4	0.2	K91
47,801.639.....	0.926	16.1	1.4	0.2	K91
47,830.608.....	0.960	16.9	0.5	0.2	K91
50,629.888.....	0.238	20.2	−0.5	1.0	KPNO
50,752.713.....	0.382	16.3	0.2	1.0	KPNO
50,934.856.....	0.596	10.5	0.7	1.0	KPNO
50,981.966.....	0.651	8.3	−0.6	1.0	KPNO
51,051.755.....	0.732	8.0	−0.7	1.0	KPNO
51,106.757.....	0.797	10.0	0.4	1.0	KPNO
51,301.995.....	0.026	19.3	−0.2	1.0	KPNO
51,346.940.....	0.078	20.5	−0.7	1.0	KPNO
51,362.939.....	0.097	22.3	0.7	1.0	KPNO

[a] (K91) Kenyon et al. 1991; (KPNO) this paper.

the M giant behind the hot component, as computed with our final orbital elements.

Assuming a period of 1262 days, we have computed separate orbits for the 17 velocities measured by Dumm et al. (1998) and our 11 KPNO velocities. Those two sets of orbital elements are compared in Table 9. The two center-of-mass velocities are in good agreement. Given that we have only 11 KPNO velocities, the other elements of the two solutions are generally consistent with each other, although their errors do not usually overlap.

Garcia (1986) published five velocities of BX Mon, which were obtained at a wavelength of about 5200 Å. Dumm et al. (1998) showed that those velocities did not fit their orbit of the M giant. They suggested that the velocities of Garcia (1986) were contaminated by blending from lines of both components. The situation for Garcia's (1986) velocities did not improve when they were compared with M-giant orbits having a period of 1262 days. Four of the five velocities have very large positive residuals, and so Garcia's (1986) velocities were not used to improve the orbital elements.

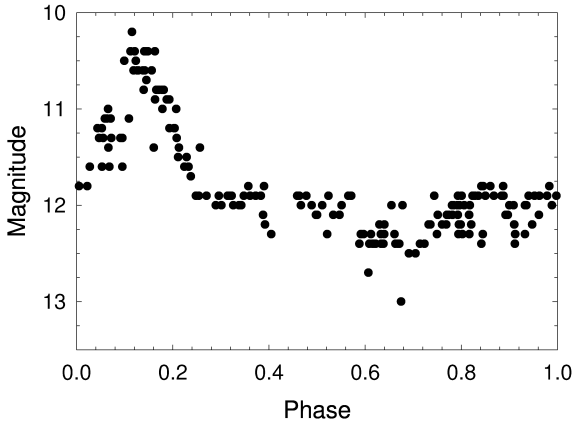

FIG. 6.—RASNZ visual observations of BX Mon plotted modulo $P = 1302$ days. Zero phase is a time of conjunction with the M giant behind the hot component, as computed from our final spectroscopic orbit.

From a comparison of the variances of the velocities for the two orbits, our velocities have been given weights of 0.33 relative to those of Dumm et al. (1998), and no zero-point velocity correction was made. In a single solution of all 28 velocities, however, the mean residual of our KPNO velocities was nearly −0.5 km s^{-1}. Thus, with 0.5 km s^{-1} added to the KPNO velocities, a final solution of the combined data was computed with SB1. The final period of 1259 days as well as the other orbital elements are given in Table 9, while the velocities and the residuals to the final orbit are listed in Table 8. Figure 7 compares the observed velocities with the computed velocity curve, where zero phase is a time of periastron passage.

7. RS OPHIUCHI

7.1. *Brief Orbital History*

From echelle spectroscopic observations at 5200 Å, Dobrzycka & Kenyon (1994) obtained 47 cross-correlation

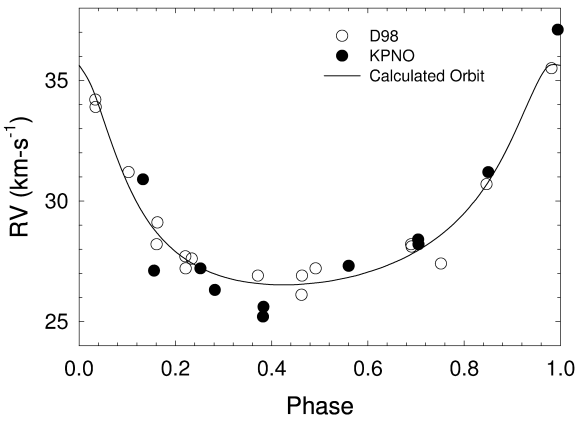

FIG. 7.—Same as Fig. 5, but for BX Mon

TABLE 7

ORBITAL ELEMENTS OF CI CYGNI

Parameter	Kenyon et al. 1991	KPNO-Data Solution	Final Solution
P (days).....	855.25 (fixed)	855.25 (fixed)	853.8 ± 2.9
T (HJD).....	...	...	$2{,}450{,}426.4 \pm 59.6$
T_0 (HJD).....	...	$2{,}450{,}570.4 \pm 11.2$	...
γ (km s^{-1}).....	18.4 ± 0.4	15.2 ± 0.3	14.96 ± 0.23
K_1 (km s^{-1}).....	7.0 ± 0.5	6.7 ± 0.4	6.70 ± 0.30
e.....	0.0	0.0	0.109 ± 0.048
ω_1 (deg)	...	...	297.7 ± 24.7
$a_1 \sin i$ (km)	$78.8 \pm 9.4 \times 10^6$	$78.9 \pm 4.7 \times 10^6$	$78.2 \pm 3.5 \times 10^6$
$f(m)$	0.027 ± 0.010	0.027 ± 0.005	0.0262 ± 0.0035

velocities of the cool giant. Many spectra of RS Oph also showed features of a hot A-type spectrum, and Dobrzycka & Kenyon (1994) determined velocities of that component by cross-correlating the spectra with an A-type template.

TABLE 8

RADIAL VELOCITIES OF BX MONOCEROTIS

HJD (2,400,000+)	Phase	Velocity (km s^{-1})	$O-C$ (km s^{-1})	Weight	Source[a]
48,624.000.....	0.161	28.2	−0.5	1.00	D98
48,626.000.....	0.163	29.1	0.5	1.00	D98
48,699.000.....	0.221	27.7	0.1	1.00	D98
48,700.000.....	0.221	27.2	−0.4	1.00	D98
49,003.000.....	0.462	26.1	−0.4	1.00	D98
49,004.000.....	0.463	26.9	0.4	1.00	D98
49,040.000.....	0.491	27.2	0.6	1.00	D98
49,290.000.....	0.690	28.2	0.4	1.00	D98
49,291.000.....	0.691	28.1	0.3	1.00	D98
49,368.000.....	0.752	27.4	−1.2	1.00	D98
49,487.000.....	0.846	30.7	0.0	1.00	D98
49,657.000.....	0.981	35.5	−0.2	1.00	D98
49,723.000.....	0.034	34.2	−0.1	1.00	D98
49,724.000.....	0.035	33.9	−0.4	1.00	D98
49,810.000.....	0.103	31.2	0.6	1.00	D98
49,975.000.....	0.234	27.6	0.2	1.00	D98
49,997.967.....	0.252	27.2	0.0	0.33	KPNO
50,148.000.....	0.371	26.9	0.3	1.00	D98
50,161.655.....	0.382	25.2	−1.4	0.33	KPNO
50,162.669.....	0.383	25.6	−1.0	0.33	KPNO
50,386.045.....	0.560	27.3	0.5	0.33	KPNO
50,567.670.....	0.705	28.4	0.5	0.33	KPNO
50,568.649.....	0.705	28.2	0.2	0.33	KPNO
50,750.996.....	0.850	31.2	0.4	0.33	KPNO
50,932.649.....	0.994	37.1	1.4	0.33	KPNO
51,106.974.....	0.133	30.9	1.4	0.33	KPNO
51,135.914.....	0.156	27.1	−1.7	0.33	KPNO
51,294.676.....	0.282	26.3	−0.7	0.33	KPNO

[a] (D98) Dumm et al. 1998; (KPNO) this paper.

They found a period of 460 days from both sets of velocities and preferred a circular-orbit solution for the cool giant. Dobrzycka & Kenyon (1994) examined several possibilities for the source of the A-type spectrum, including one that assumes that the velocities of the A-type spectra result from orbital motion of a companion. They concluded that the computed masses of the components of RS Oph are more reasonable if it is considered to be just a single-lined binary.

7.2. *Orbital Elements*

From 1995 October to 1999 July, we obtained 15 radial velocities of RS Oph (see Table 10). Assuming a period of 460 days, preliminary orbital elements were computed with BISP and all elements were refined with SB1. Then SB1C was used to obtain a circular-orbit solution. In Table 11 that solution is compared with the circular solution given by Dobrzycka & Kenyon (1994). While the periods and center-of-mass velocities of the two solutions are similar, our semiamplitude is over 50% larger. However, velocities of both sets have relatively large residuals to their respective orbits, and the orbit of Dobrzycka & Kenyon (1994) has no velocities near phase minimum.

Both sets of velocities are less precise that those of other observed symbiotic stars. Dobrzycka & Kenyon (1994) stated that some of their spectra correlated better with an A-type template rather than with an M-type template. Our larger than usual velocity uncertainties may be attributable, in part, to the lower signal-to-noise ratio of the spectra (see Fig. 1) since RS Oph is one of the faintest stars on our program. In addition, RS Oph was often observed at large hour angles, which may have resulted in poorer guiding of the star on the spectrograph slit. Despite such problems, we decided to combine the velocities into a single solution. As a result of a comparison of the two circular-orbit solutions, no zero-point shift was added to either set of velocities. From a comparison of the variances of the velocities of the

TABLE 9

ORBITAL ELEMENTS OF BX MONOCEROTIS

Parameter	Dumm et al. 1998	KPNO-Data Solution	Final Solution
P (days).....	1262 (fixed)	1262 (fixed)	1259 ± 16
T (HJD).....	$2{,}449{,}680 \pm 16$	$2{,}451{,}024 \pm 43$	$2{,}449{,}680 \pm 17$
γ (km s^{-1}).....	29.1 ± 0.1	29.0 ± 0.4	29.12 ± 0.13
K_1 (km s^{-1}).....	4.4 ± 0.2	6.7 ± 1.6	4.61 ± 0.24
e.....	0.45 ± 0.04	0.55 ± 0.14	0.444 ± 0.037
ω_1 (deg)	10 ± 5	34 ± 9	11.8 ± 5.5
$a_1 \sin i$ (km)	$68 \pm 4 \times 10^6$	$97 \pm 26 \times 10^6$	$71.5 \pm 4.0 \times 10^6$
$f(m)$	0.008 ± 0.001	0.023 ± 0.018	0.0092 ± 0.0015

TABLE 10

RADIAL VELOCITIES OF RS OPHIUCHI

HJD (2,400,000+)	Phase	Velocity (km s^{-1})	$O-C$ (km s^{-1})	Weight	Source[a]
45,035.038.....	0.767	−41.0	−2.6	0.5	DK94
45,063.017.....	0.829	−32.0	0.3	0.5	DK94
45,063.963.....	0.831	−35.0	−2.9	0.5	DK94
45,097.923.....	0.905	−27.4	−1.0	0.5	DK94
45,426.977.....	0.627	−41.1	10.8	0.5	DK94
45,426.993.....	0.627	−41.6	10.3	0.5	DK94
45,513.743.....	0.818	−36.6	−3.3	0.5	DK94
46,538.993.....	0.067	−29.0	−4.0	0.5	DK94
46,540.952.....	0.072	−32.0	−6.8	0.5	DK94
46,602.834.....	0.207	−40.7	−4.9	0.5	DK94
46,605.743.....	0.214	−39.3	−2.8	0.5	DK94
46,608.764.....	0.220	−39.4	−2.3	0.5	DK94
46,635.720.....	0.280	−37.6	5.7	0.5	DK94
46,691.608.....	0.402	−54.1	−0.2	0.5	DK94
46,867.010.....	0.787	−38.0	−1.6	0.5	DK94
46,891.957.....	0.842	−34.9	−3.8	0.5	DK94
46,895.953.....	0.851	−33.9	−3.6	0.5	DK94
46,918.913.....	0.901	−32.2	−5.6	0.5	DK94
46,929.994.....	0.925	−27.7	−2.4	0.5	DK94
46,953.833.....	0.978	−23.5	0.2	0.5	DK94
46,979.733.....	0.034	−25.8	−1.9	0.5	DK94
47,312.835.....	0.765	−39.3	−0.7	0.5	DK94
47,313.822.....	0.768	−38.6	−0.2	0.5	DK94
47,486.561.....	0.147	−38.2	−8.1	0.5	DK94
47,719.764.....	0.658	−59.2	−9.9	0.5	DK94
47,777.656.....	0.785	−36.0	0.5	0.5	DK94
47,787.583.....	0.807	−37.4	−3.0	0.5	DK94
47,811.576.....	0.860	−30.5	−0.9	0.5	DK94
47,967.019.....	0.201	−29.5	5.6	0.5	DK94
47,992.928.....	0.258	−43.9	−2.9	0.5	DK94
48,016.933.....	0.310	−44.5	1.9	0.5	DK94
48,048.826.....	0.380	−54.3	−1.9	0.5	DK94
48,349.954.....	0.041	−22.8	1.3	0.5	DK94
48,368.857.....	0.083	−21.2	4.5	0.5	DK94
48,400.832.....	0.153	−20.1	10.5	0.5	DK94
48,411.892.....	0.177	−30.3	2.5	0.5	DK94
48,429.805.....	0.216	−38.5	−1.8	0.5	DK94
48,695.025.....	0.798	−39.5	−4.3	0.5	DK94
48,723.000.....	0.860	−30.6	−1.0	0.5	DK94
48,754.922.....	0.930	−28.6	−3.5	0.5	DK94
48,782.831.....	0.991	−34.3	−10.8	0.5	DK94
48,816.771.....	0.065	−29.5	−4.6	0.5	DK94
48,872.718.....	0.188	−34.5	−0.6	0.5	DK94
48,909.584.....	0.269	−44.4	−2.2	0.5	DK94
49,106.948.....	0.702	−42.8	2.4	0.5	DK94
49,136.907.....	0.768	−36.6	1.7	0.5	DK94
49,174.784.....	0.851	−30.4	−0.1	0.5	DK94
49,998.639.....	0.659	−49.1	0.2	1.0	KPNO
50,162.905.....	0.019	−18.0	5.6	1.0	KPNO
50,254.723.....	0.221	−33.5	3.7	1.0	KPNO
50,320.643.....	0.365	−48.5	2.8	1.0	KPNO
50,387.593.....	0.512	−61.9	−5.0	1.0	KPNO
50,568.854.....	0.910	−27.5	−1.4	1.0	KPNO
50,627.799.....	0.039	−19.3	4.7	1.0	KPNO
50,751.574.....	0.311	−49.6	−3.1	1.0	KPNO
50,933.851.....	0.711	−42.1	2.2	1.0	KPNO
50,981.817.....	0.816	−27.5	6.0	1.0	KPNO
50,983.747.....	0.820	−26.8	6.3	1.0	KPNO
51,051.677.....	0.970	−19.7	4.1	1.0	KPNO
51,106.592.....	0.090	−27.4	−1.3	1.0	KPNO
51,294.889.....	0.503	−63.5	−6.6	1.0	KPNO
51,363.664.....	0.654	−45.1	4.6	1.0	KPNO

[a] (DK94) Dobrzycka & Kenyon 1994; (KPNO) this paper.

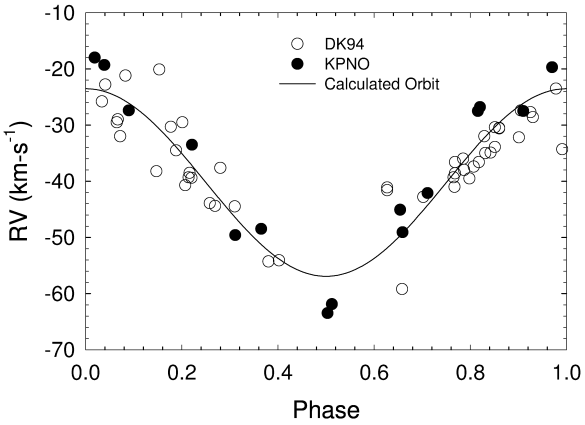

FIG. 8.—Same as Fig. 3, but for RS Oph

two solutions, the velocities of Dobrzycka & Kenyon (1994) were given weights of 0.5 relative to ours.

Combining the two sets of velocities, we computed both eccentric and circular orbits. According to the precepts of Lucy & Sweeney (1971), the circular orbit is to be preferred, and that orbit is listed in Table 11. The velocities and velocity residuals are given in Table 10. Figure 8 compares the radial velocities with the computed velocity curve. Zero phase is T_0, a time of maximum positive velocity.

8. AG PEGASI

8.1. *Brief Orbital History*

From several decades of monitoring, Merrill (1951, 1959) found velocity variations of about 800 days for various metallic and hydrogen emission lines in the spectrum of AG Peg. Hutchings, Cowley, & Redman (1975) adopted a period of 820 days and used 23 absorption-line velocities to determine both a circular- and an eccentric-orbit solution. The best current orbit is that of Kenyon et al. (1993), who obtained 58 additional velocities, nine obtained at McDonald Observatory and 49 with telescopes of the SAO. They determined a spectroscopic period of 812.3 days, which they noted is in excellent agreement with the 816.5 days photometric period of Fernie (1985). Their velocities, combined with those used by Hutchings et al. (1975), appeared to rule out eccentricities as large as 0.10–0.25, and Kenyon et al. (1993) favored a circular-orbit solution.

8.2. *Orbital Elements*

From 1996 October to 1999 July, we obtained 13 radial velocities of AG Peg (see Table 12). Assuming the spectroscopic period of Kenyon et al. (1993), we obtained preliminary elements with BISP and refined them with SB1. In Table 13, our elements are compared with those from the eccentric solution of Kenyon et al. (1993). The center-of-mass velocities are identical, while the semiamplitudes agree to within their errors. Thus, we combined our velocities with the various sets of velocities used by Kenyon et al. (1993).

To compare the velocity offsets and determine the weights for the velocities of the various data sets, we first computed an eccentric-orbit solution of the 49 SAO velocities alone. Four other sets of velocities were compared with this solution: (1) eight remeasured velocities from plates obtained by Merrill (Hutchings et al. 1975), (2) twelve

TABLE 11

ORBITAL ELEMENTS OF RS OPHIUCHI

Parameter	Dobrzycka & Kenyon 1994	KPNO-Data Solution	Final Solution
P (days).....	460 ± 5	447 ± 4	455.72 ± 0.83
T_0 (HJD)	$2{,}450{,}114.9 \pm 11.2$	$2{,}451{,}502 \pm 9$	$2{,}450{,}154.1 \pm 4.6$
γ (km s^{-1}).....	-38.9 ± 1.2	-39.6 ± 0.8	-40.22 ± 0.64
K_1 (km s^{-1}).....	12.8 ± 2.0	20 ± 1	16.71 ± 0.97
e	0.0	0.0	0.0
ω_1 (deg)	...	...	...
$a_1 \sin i$ (km)	...	$123 \pm 7 \times 10^6$	$104.7 \pm 6.1 \times 10^6$
$f(m)$	...	0.37 ± 0.06	0.221 ± 0.038

velocities of Cowley & Stencel (1973), (3) three velocities of Hutchings et al. (1975), and (4) nine velocities of Slovak (Kenyon et al. 1993). From an examination of the mean velocity residuals for the various data sets, 1.3 km s^{-1} was added to all velocities of Cowley & Stencel (1973). From a comparison of variances, weights of 0.1, 0.1, 0.4, and 0.75 were assigned to the remeasured velocities of Merrill's plates, the velocities of Cowley & Stencel, those of Slovak, and the SAO velocities, respectively. The three velocities of Hutchings et al. (1975) had large residuals and were not included in our final solutions.

With the above 91 velocities appropriately weighted, we computed eccentric- and circular-orbit solutions using SB1 and SB1C. According to the precepts of Lucy & Sweeney (1971), the eccentric-orbit solution is to be preferred, and it is listed in Table 13. We note that within their errors the values of the periods, semiamplitudes, and mass functions are the same for the two solutions. The velocities and velocity residuals from the computed orbit are given in Table 12. Figure 9 compares the velocities with the computed velocity curve, where zero phase is a time of periastron passage.

9. DISCUSSION

Except in the case of BX Mon, our velocities of the late-type giant in the six symbiotic binaries are at least as precise if not superior, as judged by the variances of the velocities in comparable solutions, to velocities obtained by previous observers at shorter wavelengths. Comparison with numerous SAO velocities is available for four of the six binaries. In those cases, the weights of the SAO velocities, based on variances, range from 0.2–0.75 relative to the KPNO velocities. The six symbiotic stars discussed in this paper have reasonably well determined orbits in the literature. The agreement of our independent orbital solutions with published results generally confirms the previous orbital solutions and demonstrates the validity of using infrared velocities to determine the orbits of the late-type giants in symbiotic systems.

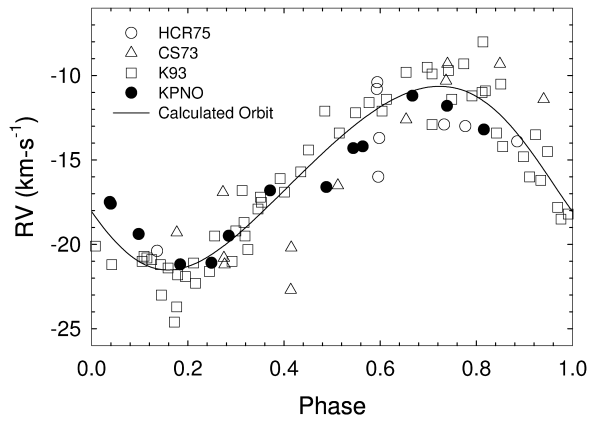

FIG. 9.—Same as Fig. 5, but for AG Peg

In a binary system, tidal forces will tend to circularize the orbit over the course of the stars' evolution (Zahn 1977). Since symbiotic systems are extensively evolved, typically consisting of an M giant and a white dwarf, we might expect most systems to have circular orbits. However, since symbiotic systems are mass-exchange binaries, it is possible that the M-giant component fills a substantial fraction of its Roche lobe and may be tidally distorted. Sterne (1941) showed that the effects of tidal distortion can produce an orbit with a spurious eccentricity and an expected longitude of periastron, ω, of 90° or 270°. We have determined circular orbits for three systems, EG And, T CrB, and RS Oph, all having periods less than 500 days. On the other hand, for BX Mon, the system with the longest period, 1259 days, the orbit is clearly eccentric. The remaining two systems, CI Cyg and AG Peg, have intermediate orbital periods of 800–900 days and low eccentricities of ~ 0.1.

Is there evidence for tidal distortion in any of the circular or low-eccentricity systems? Although assuming a circular orbit for T CrB, Kenyon & Garcia (1986) also obtained an eccentric-orbit solution ($e = 0.012 \pm 0.005$, $\omega = 80° \pm 6°$), which they noted slightly improved the fit to their radial velocities. They argued that the eccentricity is spurious, resulting from the ellipsoidal nature of the M giant. Belczyński & Mikolajewska (1998) concurred with that assessment. They computed a rough value for the predicted spurious eccentricity, compared it and the expected value of ω with the eccentric-orbit solution of Kenyon & Garcia (1986), and concluded that the small eccentricity was very likely due to tidal effects. For our final eccentric-orbit solution of T CrB, the eccentricity and ω are 0.0041 ± 0.0076 and $177° \pm 68°$, respectively. Those values provide *no* evidence for tidal distortion and instead, are entirely consistent with observational errors. The circular-orbit solution passes the tests of Lucy & Sweeney (1971) by a wide margin.

For CI Cyg and AG Peg, our final eccentric-orbit values of ω are $298° \pm 25°$ and $112° \pm 22°$, respectively. Considering the errors, the computed values of ω nearly encompass the expected spurious values, giving possible support to the argument that the eccentricities of ~ 0.1 are spurious. Previously, for CI Cyg Kenyon et al. (1991) found $\omega = 309° \pm 28°$ and concluded that this was probably the result of tidal distortion of the red giant. Although additional precise radial velocities may well tilt the balance in favor of circular orbits, the eccentric-orbit solutions have been retained for these two stars. Orbits for additional sym-

TABLE 12

RADIAL VELOCITIES OF AG PEGASI

HJD (2,400,000+)	Phase	Velocity (km s^{-1})	$O-C$ (km s^{-1})	Weight	Source[a]
31,753.690.....	0.596	−16.0	−4.1	0.10	HCR75
31,754.620.....	0.598	−13.7	−1.8	0.10	HCR75
32,719.980.....	0.777	−13.0	−2.1	0.10	HCR75
32,807.900.....	0.885	−13.9	−0.5	0.10	HCR75
33,501.860.....	0.733	−12.9	−2.3	0.10	HCR75
34,649.760.....	0.136	−20.4	1.1	0.10	HCR75
35,023.680.....	0.593	−10.8	1.2	0.10	HCR75
35,024.710.....	0.594	−10.4	1.6	0.10	HCR75
37,955.740.....	0.177	−19.3	2.2	0.10	CS73
38,036.620.....	0.275	−20.8	−0.7	0.10	CS73
39,048.650.....	0.512	−16.5	−2.7	0.10	CS73
39,398.710.....	0.940	−11.4	4.2	0.10	CS73
39,786.630.....	0.414	−22.7	−6.3	0.10	CS73
39,787.580.....	0.415	−20.2	−3.8	0.10	CS73
40,142.620.....	0.849	−9.3	3.0	0.10	CS73
40,489.700.....	0.273	−16.9	3.2	0.10	CS73
40,491.660.....	0.276	−21.2	−1.1	0.10	CS73
40,868.750.....	0.737	−10.3	0.3	0.10	CS73
40,871.590.....	0.740	−9.3	1.4	0.10	CS73
41,619.610.....	0.654	−12.6	−1.6	0.10	CS73
43,679.900.....	0.172	−24.6	−3.1	0.40	K93
43,715.780.....	0.216	−22.3	−1.2	0.40	K93
43,799.670.....	0.319	−19.5	−0.5	0.40	K93
43,821.590.....	0.346	−17.9	0.4	0.40	K93
43,866.550.....	0.401	−16.9	−0.1	0.40	K93
44,032.900.....	0.604	−12.1	−0.3	0.40	K93
44,117.840.....	0.708	−12.9	−2.2	0.40	K93
44,442.920.....	0.105	−21.0	0.1	0.40	K93
44,602.560.....	0.300	−19.2	0.3	0.40	K93
45,840.851.....	0.814	−8.0	3.5	0.75	K93
45,871.781.....	0.851	−10.5	1.9	0.75	K93
45,930.714.....	0.923	−13.5	1.4	0.75	K93
45,950.646.....	0.948	−14.5	1.4	0.75	K93
46,095.458.....	0.125	−20.9	0.5	0.75	K93
46,249.760.....	0.313	−16.8	2.4	0.75	K93
46,282.608.....	0.353	−17.5	0.6	0.75	K93
46,362.551.....	0.451	−14.4	1.0	0.75	K93
46,564.834.....	0.698	−9.5	1.2	0.75	K93
46,600.839.....	0.742	−9.7	1.0	0.75	K93
46,626.686.....	0.774	−9.3	1.6	0.75	K93
46,657.649.....	0.812	−11.0	0.4	0.75	K93
46,682.716.....	0.842	−13.4	−1.3	0.75	K93
46,757.432.....	0.934	−16.2	−0.9	0.75	K93
46,786.477.....	0.969	−17.8	−1.0	0.75	K93
46,804.439.....	0.991	−18.2	−0.5	0.75	K93
46,928.854.....	0.143	−21.2	0.3	0.75	K93
46,957.803.....	0.179	−21.8	−0.3	0.75	K93
47,020.673.....	0.256	−19.5	1.0	0.75	K93
47,070.608.....	0.317	−18.7	0.4	0.75	K93
47,098.568.....	0.351	−17.2	1.0	0.75	K93
47,132.459.....	0.392	−16.1	0.9	0.75	K93
47,167.438.....	0.435	−15.7	0.1	0.75	K93
47,346.918.....	0.654	−9.8	1.2	0.75	K93
47,390.783.....	0.708	−9.9	0.8	0.75	K93
47,424.660.....	0.749	−11.4	−0.7	0.75	K93
47,458.587.....	0.791	−11.2	−0.1	0.75	K93
47,481.559.....	0.819	−10.9	0.7	0.75	K93
47,511.452.....	0.855	−14.2	−1.7	0.75	K93
47,546.493.....	0.898	−14.8	−0.9	0.75	K93
47,718.833.....	0.109	−20.7	0.5	0.75	K93
47,748.802.....	0.145	−23.0	−1.5	0.75	K93
47,774.785.....	0.177	−23.7	−2.2	0.75	K93
47,803.566.....	0.212	−21.1	0.1	0.75	K93
47,830.483.....	0.245	−21.6	−0.9	0.75	K93

TABLE 12—*Continued*

HJD (2,400,000+)	Phase	Velocity (km s^{-1})	$O-C$ (km s^{-1})	Weight	Source[a]
47,868.461.....	0.292	−21.0	−1.3	0.75	K93
47,895.474.....	0.325	−20.3	−1.4	0.75	K93
48,026.860.....	0.485	−12.1	2.4	0.75	K93
48,050.817.....	0.515	−13.4	0.3	0.75	K93
48,078.809.....	0.549	−12.2	0.7	0.75	K93
48,101.759.....	0.577	−11.6	0.7	0.75	K93
48,131.677.....	0.613	−11.4	0.2	0.75	K93
48,374.875.....	0.911	−16.0	−1.6	0.75	K93
48,428.791.....	0.976	−18.5	−1.4	0.75	K93
48,454.739.....	0.008	−20.1	−1.7	0.75	K93
48,482.678.....	0.042	−21.2	−1.6	0.75	K93
48,542.526.....	0.115	−20.8	0.5	0.75	K93
48,578.508.....	0.159	−21.4	0.1	0.75	K93
48,607.455.....	0.195	−21.9	−0.5	0.75	K93
50,387.670.....	0.371	−16.8	0.8	1.00	KPNO
50,629.931.....	0.667	−11.2	−0.3	1.00	KPNO
50,688.916.....	0.739	−11.8	−1.1	1.00	KPNO
50,751.755.....	0.816	−13.2	−1.7	1.00	KPNO
50,933.941.....	0.038	−17.5	2.0	1.00	KPNO
50,934.996.....	0.040	−17.6	1.9	1.00	KPNO
50,982.856.....	0.098	−19.4	1.6	1.00	KPNO
51,052.935.....	0.184	−21.2	0.2	1.00	KPNO
51,106.639.....	0.249	−21.1	−0.5	1.00	KPNO
51,135.735.....	0.285	−19.5	0.4	1.00	KPNO
51,301.978.....	0.488	−16.6	−2.2	1.00	KPNO
51,347.882.....	0.544	−14.3	−1.3	1.00	KPNO
51,363.871.....	0.564	−14.2	−1.6	1.00	KPNO

[a] (HCR75) Hutchings et al. 1975; (CS73) Cowley & Stencel 1973; (K93) Kenyon et al. 1993; (KPNO) this paper.

biotic systems will provide data that can be used to statistically examine the period-eccentricity distribution of symbiotic systems.

The mass functions computed from the final orbital elements represent the minimum masses of the hot components. For four of the systems, EG And, CI Cyg, BX Mon, and AG Peg, the mass function is quite small, 0.01–0.03. Such small values can result from typical white-dwarf mass secondaries, roughly 0.6 $M_\odot$, with assumed M-giant primary masses of 1–2 $M_\odot$. Minimum masses of the hot companions to T CrB and RS Oph are much larger, 0.32 and 0.22, respectively. These large mass functions are also consistent with white-dwarf secondaries. For T CrB, Belczyński & Mikolajewska (1998) and Hachisu & Kato (1999) argued various lines of reasoning that suggest a white dwarf with a mass of about 1.0–1.4 $M_\odot$. For RS Oph, a white dwarf with a mass of about 1.2 $M_\odot$ has been considered (Dobrzycka & Kenyon 1994; Shore et al. 1996; Dobrzycka et al. 1996). However, arguments also can be made that the large mass-function systems contain main-sequence accretors (Kenyon et al. 1991; Dobrzycka et al. 1996). The current evolutionary scenario for symbiotic binaries includes a short-lived phase with a main-sequence accretor (Iben & Tutkov 1996). Future papers of the current series will increase the number of symbiotic systems with good orbital parameters. This should provide a statistical limit on the number of possible main-sequence accretors.

We thank G. W. Henry for helpful discussions and U. Munari and T. Dumm for providing information about their published radial-velocity observations The help of T. Dumm, who forwarded the RASNZ visual observations, is appreciated. We are grateful to the National Optical Astronomy Observatories director, S. Wolff, for supporting

TABLE 13

ORBITAL ELEMENTS OF AG PEGASI

Parameter	Kenyon et al. 1993	KPNO-Data Solution	Final Solution
P (days)	812.3 ± 6.3	812.3 (fixed)	818.2 ± 1.6
T (HJD)	...	2,450,984 ± 81	2,446,812 ± 48
γ (km s^{-1})	−16.0 ± 0.5	−16.0 ± 0.3	−15.86 ± 0.15
K_1 (km s^{-1})	5.3 ± 0.6	4.4 ± 0.4	5.44 ± 0.20
e	0.12 ± 0.13	0.16 ± 0.11	0.110 ± 0.039
ω_1 (deg)	85 ± 60	136 ± 39	112 ± 22
$a_1 \sin i$ (km)	...	48 ± 5 × 10^6	60.8 ± 2.3 × 10^6
$f(m)$	...	0.007 ± 0.002	0.0135 ± 0.0015

our use of the NICMASS array at the Kitt Peak National Observatory. We thank the referee for helpful suggestions. This research has been supported in part by NASA grants NCC 5-228 and NCC 5-96 and by NSF grant HRD 97-06268 to Tennessee State University. This research has made use of the SIMBAD database, operated at CDS, Strasbourg, France, as well as NASA's Astrophysics Data System Abstract Service.

REFERENCES

Aller, L. H. 1954, Publ. Dom. Astrophys. Obs. Victoria, 9, 321
Barker, E. S., Evans, D. S., & Laing, J. D. 1967, R. Obs. Bull., No. 130
Batten, A. H., Fletcher, J. M., & MacCarthy, D. G. 1989, Publ. Dom. Astrophys. Obs. Victoria, 17, 1
Belczyński, K., & Mikolajewska, J. 1998, MNRAS, 296, 77
Belyakina, T. S. 1979, Izv. Krymskoi Astrofiz. Obs., 59, 133
———. 1984, Izv. Krymskoi Astrofiz. Obs., 68, 108
Berman, L. 1932, PASP, 44, 318
Chakrabarty, D., & Roche, P. 1997, ApJ, 489, 254
Cowley, A., & Stencel, R. 1973, ApJ, 184, 687
Dobrzycka, D., & Kenyon, S. J. 1994, AJ, 108, 2259
Dobrzycka, D., Kenyon, S. J., Proga, D., Mikolajewska, J., & Wade, R. A. 1996, AJ, 111, 2090
Dumm, T., Mürset, U., Nussbaumer, H., Schild, H., Schmid, H. M., Schmutz, W., & Shore, S. N. 1998, A&A, 336, 637
Fernie, J. D. 1985, PASP, 97, 653
Fitzpatrick, M. J. 1993, in ASP Conf. Ser. 52, Astronomical Data Analysis Software and Systems II, ed. R. J. Hanisch, R. V. J. Brissenden, & J. Barnes (San Francisco: ASP), 472
Garcia, M. R. 1986, AJ, 91, 1400
Hachisu, I., & Kato, M. 1999, ApJ, 517, L47
Hinkle, K. H., Cuberly, R. W., Gaughan, N. A., Heynssens, J. B., Joyce, R. R., Ridgway, S. T., Schmitt, P., & Simmons, J. E. 1998, Proc. SPIE, 3354, 810
Hinkle, K. H., Fekel, F. C., Johnson, D. S., & Scharlach, W. W. G. 1993, AJ, 105, 1074
Hinkle, K. H., Lebzelter, T., & Scharlach, W. W. G. 1997, AJ, 114, 2686
Hinkle, K. H., Wilson, T. D., Scharlach, W. W. G., & Fekel, F. C. 1989, AJ, 98, 1820
Hogg, F. S. 1934, Publ. AAS, 8, 14
Hutchings, J. B., Cowley, A. P., & Redman, R. O. 1975, ApJ, 201, 404
Iben, I., Jr. & Tutukov, A. V. 1996, ApJS, 105, 145
Iijima, T. 1985, A&A, 153, 35
Joyce, R. R. 1992, in ASP Conf. Ser. 23, Astronomical CCD Observing and Reduction Techniques, ed. S. Howell (San Francisco: ASP), 258
Joyce, R. R., Hinkle, K. H., Meyer, M. R., & Skrutskie, M. F. 1998, Proc. SPIE, 3354, 741
Kenyon, S. J. 1986, The Symbiotic Stars (Cambridge: Cambridge Univ. Press)
———. 1988, AJ, 96, 337
———. 1992, in IAU Symp. 151, Evolutionary Processes in Interacting Binary Stars, ed. Y. Kondo, R. F. Sistero, & R. S. Polidan (Dordrecht: Kluwer), 137
Kenyon, S. J., & Fernández-Castro, T. 1987, AJ, 93, 938
Kenyon, S. J., & Garcia, M. R. 1986, AJ, 91, 125
Kenyon, S. J., & Mikolajewska, J. 1995, AJ, 110, 391
Kenyon, S. J., Mikolajewska, J., Mikolajewska, M., Polidan, R., & Slovak, M. H. 1993, AJ, 106, 1573
Kenyon, S. J., Oliversen, N. A., Mikolajewska, J., Mikolajewska, M., Stencel, R. E., Garcia, M. R., & Anderson, C. M. 1991, AJ, 101, 637
Kenyon, S. J., & Webbink, R. F. 1984, ApJ, 279, 252
Kholopov, P. N. 1985, General Catalogue of Variable Stars (4th ed.; Moscow: Nauka)
Kraft, R. P. 1958, ApJ, 127, 625
Lucy, L. B., & Sweeney, M. A. 1971, AJ, 76, 544
Mayall, M. W. 1940, Bull. Harvard Coll. Obs., 913, 8
Merrill, P. W. 1951, ApJ, 113, 605
———. 1958, Mem. Soc. R. Sci. Liège, Ser. 4, 20, 436
———. 1959, ApJ, 129, 44
Michalitsianos, A. G., Kafatos, M., Feibelman, W. A., & Hobbs, R. W. 1982, ApJ, 253, 735
Munari, U. 1993, A&A, 273, 425
Munari, U., Margoni, R., Iijima, T. Mammano, A. 1988, A&A, 198, 173
Mürset, U., Nussbaumer, H., Schmid, H. M., & Vogel, M. 1991, A&A, 248, 458
Mürset, U., & Schmid, H. M. 1999, A&AS, 137, 473
Oliversen, N. A., Anderson, C. M., Stencel, R. E., & Slovak, M. H. 1985, ApJ, 295, 620
Plaskett, J. S. 1928, Publ. Dom. Astrophys. Obs. Victoria, 4, 119
Sanford, R. F. 1949, ApJ, 109, 81
Scarfe, C. D., Batten, A. H., & Fletcher, J. M. 1990, Publ. Dom. Astrophys. Obs. Victoria, 18, 21
Seal, P. 1997, Ap&SS, 254, 85
Seaquist, E. R., Krogulec, M., & Taylor, A. R. 1993, ApJ, 410, 260
Shore, S. N., Kenyon, S. J., Starrfield, S., & Sonneborn, G. 1996, ApJ, 456, 717
Skopal, A. 1997, A&A, 318, 53
Skopal, A., Chochol, D., Vittone, A. A., Blanco, C., & Mammano, A. 1991, A&A, 245, 531
Smith, S. E. 1980, ApJ, 237, 831
Sterne, T. E. 1941, Proc. Natl. Acad. Sci., 27, 168
Webster, B. L., & Allen, D. A. 1975, MNRAS, 171, 171
Whitelock, P. A. 1987, PASP, 99, 573
Wilson, R. E., & Vaccaro, T. R. 1997, MNRAS, 291, 54
Wolfe, R. H., Horak, H. G., & Storer, N. W. 1967, in Modern Astrophysics, ed. M. Hack (New York: Gordon & Breach), 251
Zahn, J.-P. 1977, A&A, 57, 383